Journal of Photochemistry and Photobiology A: Chemistry 214 (2010) 215–223

Contents lists available at ScienceDirect

Journal of Photochemistry and Photobiology A: Chemistry

journal homepage: www.elsevier.com/locate/jphotochem

Photo-induced treatment of breast epithelial cancer cells using nanostructured titanium dioxide solution

N. Lagopati[a,b], P.V. Kitsiou[b], A.I. Kontos[a], P. Venieratos[b], E. Kotsopoulou[b], A.G. Kontos[a], D.D. Dionysiou[c], S. Pispas[d], E.C. Tsilibary[b,*], P. Falaras[a,**]

[a] Institute of Physical Chemistry, NCSR "Demokritos", 15310, Aghia Paraskevi Attikis, Athens, Greece
[b] Institute of Biology, NCSR "Demokritos", 15310, Aghia Paraskevi Attikis, Athens, Greece
[c] Department of Civil and Environmental Engineering, University of Cincinnati, Cincinnati, OH 45221-0071, USA
[d] Theoretical and Physical Chemistry Institute, National Hellenic Research Foundation, 48 Vassileos Constantinou Ave., 11635 Athens, Greece

ARTICLE INFO

Article history:
Received 8 March 2010
Received in revised form 25 June 2010
Accepted 29 June 2010
Available online 7 July 2010

Keywords:
Breast cancer
Photocatalysis
Nanonstructured TiO_2
Apoptosis

ABSTRACT

The photo-induced bioactivity of titanium dioxide was investigated in terms of determining the conditions for photocatalytic treatment of cancer cells and also exploring the molecular mechanisms involved in this process. Cultured MCF-7 and MDA-MB-468 breast cancer epithelial cells were irradiated, using UV-A light (wavelength 350 nm) for 20 min, in the presence of nanostructured titania aqueous dispersions prepared using the sol–gel technique. Detailed characterization of the titania sols confirmed the presence of the photocatalyst in the form of anatase nanoparticles. Two different techniques were employed to examine the effects on cell cycle and the viability of the treated culture: propidium iodide (PI) flow cytometric (FACScan) assays permitted the identification of treatment effects on the cell cycle and cell viability analysis (MTT assays) allowed the definition of the precise percentage of cells that are still alive and functionable, after the treatment. A selective action of both TiO_2 nanoparticles and photocatalytically activated titania was observed on the highly malignant MDA-MB-468 cells. Upon irradiation, these cells were induced to undergo apoptotic cell death, compared to the MCF-7 cells which were still unimpaired. This was profoundly revealed via Western blot analysis. The molecular mechanism of apoptosis is associated at least in part with increase of caspase-3-mediated poly(ADP-ribose) polymerase (PARP) cleavage.

1. Introduction

Titanium is widely used in biomedical applications. Its mechanical properties and biocompatibility, conferred by a layer of oxide present on its surface, make titanium the material of choice for various implants (artificial hip and knee joints, dental prosthetics, vascular stents, heart valves, etc.). Titanium implants have also been used widely and successfully for various types of bone-anchored reconstructions. It is believed that properties of oxide films covering titanium implant surfaces are of crucial importance for successful bone integration, in particular in compromised bone sites [1]. Furthermore, the high refractive index of titanium oxide is advantageous in biosensor applications based on optical detection methods. In both the above fields of application, novel surface modification strategies leading to biointeractive interfaces (that trigger specific responses in biological systems) are continuously sought.

Additionally, titanium dioxide has been intensively studied in the last two decades for photocatalysis purposes [2–4]. In recent studies making use of TiO_2 nanoparticles, it was demonstrated that application of the photocatalytic technology has a great impact and high potential for restoring and keeping our living environment clean and safe [5–7]. It is now well established that photoexcited titanium dioxide (TiO_2) can drive various chemical reactions due to its strong oxidizing and reducing ability. Important applications were confirmed on environmental issues such us removal of pollutants from air (VOCs, NOx, odors) [4] and water (phenols, textile azo-dyes, pesticides) [8]. By a judicious balance of their photocatalytic and superhydrophylic properties, it has also been proven that titania-modified surfaces are not only able to photochemically decompose harmful substances, but can also prevent stains formation and kill bacteria and viruses thus offering, besides efficient self-cleaning, additional self-sterilisation [9–11].

Nanoparticles can affect cellular activity [12–14]. Previous studies have shown that Ti particles induce death by apoptosis in different types of cells, such as mesenchymal stem cells [15],

* Corresponding author. Tel.: +30 210 6503583; fax: +30 210 6511767.
** Corresponding author. Tel.: +30 210 6503644; fax: +30 210 6511766.
E-mail addresses: effie@bio.demokritos.gr (E.C. Tsilibary), papi@chem.demokritos.gr (P. Falaras).

1010-6030/$ – see front matter © 2010 Elsevier B.V. All rights reserved.
doi:10.1016/j.jphotochem.2010.06.031

osteoblasts [16], brain cells [17], and necrosis in fibroblasts [18]. Recently, it has been shown that ultrafine TiO_2 can cause cyto- and geno-toxicity and induce apoptosis in human lymphoblastoid cells [19]. Interestingly, the photocatalytic properties of TiO_2-mediated toxicity have been shown to eradicate cancer cells [20,21]. It is now well established that when TiO_2 nanoparticles are excited by light whose wavelength is <390 nm, the photon energy generates pairs of electrons and holes which react with atmospheric water and oxygen to yield reactive oxygen species (ROS) which have been proved to significantly damage cancer cells [22–27]. Therefore, TiO_2 nanoparticles are one of the promising photosensitizer against cancer. Though photoexcited TiO_2 nanoparticles have been proved to be very effective in a variety of cancer, many of its anti-tumor mechanisms have not been demonstrated.

Recently, intensive research efforts in our group were focused on the possible use of TiO_2 as an anticancer agent in the presence of UV light. The aim of the present study was to investigate the potential of TiO_2 nanoparticles to induce cellular modifications characteristic for apoptosis and/or necrosis specifically in cancer cells. The cell toxicity of photo-activated-TiO_2 nanoparticles was assessed in two cancer cell lines, the MDA-MB-468 and the MCF-7, both derived from breast epithelium. Cells were exposed to nanostructured titania aqueous dispersions, prepared using the sol–gel technique. We studied the induction of cell death employing the flow cytometry based method: DNA quantification by propidium iodide (PI), the cell viability analysis (MTT) assay and western blot analysis of caspase-3-mediated PARP cleavage. We report here, that both TiO_2 nanoparticles and photoexcited TiO_2 nanoparticles exert a significant apoptotic effect especially in the highly malignant MDA-MB-468 cancer cells.

2. Materials and methods

2.1. Cell culture

Human breast epithelial cells (MCF-7 and MDA-MB-468) were cultured in 75 cm^2 flasks, in Dulbecco's modified Eagle's medium (DMEM) supplemented with 10% fetal bovine serum (FBS), 1% L-glutamine, 1% sodium pyruvate and antibiotics (all media were purchased from Biochrom Seromed, Berlin, Germany), and incubated at 37 °C, in a 5% CO_2 incubator. Also, trypsin–EDTA: 0.05%/0.02% (w/v) (Gibco BRL, Life Technologies) were used for the trypsinization of cells.

2.2. Preparation and characterizations of the TiO_2 sol

To prepare the titania material, the sol–gel technique was used [1]. Titanium (IV) tetrabutyl orthotitanate (15 ml) (Aldrich 97%) was slowly added into 100 ml of 0.2 M nitric acid solution (HNO_3, Carlo Erba) and the resulting white colloidal dispersion was rigorously stirred for 4 h, after which the solution became completely transparent showing remarkable stability. The optical transmission spectra were recorded on a Hitachi 3010 spectrophotometer in the wavelength range 300–500 nm by inserting the sol into 10 mm pathway quartz cells. Attempts to characterize the titania particles in the liquid colloidal solution by Raman scattering were not successful. Thus we covered a glass petri dish with sol droplets and left them to dry forming a titania film, white in color. Then micro-Raman spectra were measured employing an InVia Renishaw Raman spectrometer, equipped with a charge coupled device for signal detection. Excitation was performed with a 514.5 nm Argon ion laser, applying a power of about 0.2 mW on a 1 μm diameter spot of the film. Dynamic light scattering (DLS) measurements were performed on aged titania sols (10 days after preparation) after filtering the solutions through a 0.45 μm millipore filter. An ALV/CGS-3 compact goniometer system (ALV GmbH, Germany) was used, equipped with a He–Ne laser, operating at 632.8 nm, which is interfaced with an ALV-5000/EPP multi-tau digital correlator with 288 channels and an ALV/LSE-5003 light scattering electronics unit for stepper motor drive and limit switch control. Measurements were carried out at scattering angles of 90°, 45° and 135°. Average light scattering intensity from solutions was recorded and autocorrelation functions were analyzed in order to obtain the apparent hydrodynamic radii R_h as described in Ref. [28].

2.3. DNA quantification: propidium iodide (PI) staining and flow cytometry (FACScan)

For the FACScan assays, MCF-7 and MDA-MB-468 breast epithelial cells (1,000,000–2,000,000 cells) were seeded in 10 cm-dishes at a density $1–2 \times 10^6$ cells, using Dulbecco's modified Eagle's medium (DMEM) with 10% fetal bovine serum, 1% glutamine and 1% sodium pyruvate. In a series of experiments, the cell starting number is 1×10^6 cells, for all experimental conditions. In another series of experiments the starting number is 2×10^6 cells. Cells were incubated at 37 °C, 5% CO_2. They were allowed a 24-h doubling time. Then the sol was added in the media, the samples were irradiated in a laboratory constructed photocatalytic reactor, using UV-A light for 20 min and further cultured for 48 h. The reactor was equipped with four F15W/T8 black light tubes (Sylvania GTE), presenting maximum emission at 350 nm and a power density of 71.7 μW cm^{-2} on the irradiated surface. The addition of a very small amount of TiO_2 sol (~20 μl) in 1.5 ml cell culture medium (pH 7) did not alter the pH of the medium.

Propidium iodide (PI) with a flow cytometric (FACScan) assay was employed to check the effects on the cell cycle. At the end of the exposure period (48 h) the cells were treated with pepsin and suspended in a solution of 15% FBS (fetal bovine serum) and 85% PBS, and cells were centrifuged at $200 \times g$ (1200 rpm) for 10 min at room temperature. Then the cells were washed twice in 10 ml PBS and counted with a hemocytometer. The cells were in sequence resuspended in 5 ml PBS and centrifuged again. The supernatant was removed and the cells were fixed by adding 70% cold ethanol and 30% PBS (1 ml totally) and stored at −20 °C overnight. The following day the cells were centrifuged at $400 \times g$ (1400 rpm) for 5 min. The supernatant was removed, and the cells were washed (in 5 ml PBS) and centrifuged again. The next step included transferring cells into the FACS tubes, using the staining solution (20 μg/ml propidium iodide (PI), 200 μg/ml RNase in PBS for a total volume of 1.5 ml for each sample). The cells were left for 30 min at room temperature, in the dark. PI is a fluorogenic compound which is capable of binding to DNA thus labeling it. Hence the fluorescence emission was anticipated to be proportional to the DNA content of cells. The percentage of the fluorogenic cells was measured by flow cytometry (FACScan, Beckton-Dickinson, 617 nm – emission wavelength, 535 nm absorption wavelength) [29]. Experiments were repeated at least four times in duplicates. Analysis of the results showed that the starting cell density (1×10^6 or 2×10^6 cells) in each set of experiments had no effect on the obtained results.

2.4. Cell viability analysis (MTT assay)

To check the cell viability, the MTT assay protocol was used. The MTT assay [30] is based on the ability of a mitochondrial dehydrogenase enzyme from viable cells to cleave the tetrazolium rings of the pale yellow MTT and form dark blue formazan crystals which are largely impermeable to cell membranes, thus resulting in crystal accumulation within healthy cells. Solubilization of the cells by addition of a detergent results in the liberation of the crystals which then become solubilized. The number of surviving cells is directly proportional to the level of the formazan product created.

The color can then be quantified using a simple colorimetric assay. The results can be read on a multiwell scanning spectrophotometer (ELISA reader) [31].

On the day of the viability assay, the medium was removed and fresh medium was added (~100 μl/well). Furthermore, 10 μl of 3-(4,5-dimethylthiazol-2-yl)-2,5-diphenyl-terazolium bromide (MTT) solution [5 mg/ml in phosphate-buffered-saline (PBS)] was added to each well. The contents were incubated at 37 °C for at least 3 h. At the end of the incubation period, 110 μl of medium and MTT solution were removed from each well and 100 μl of dimethyl sulfoxide (DMSO) were added slowly. Then the 96-well plates were gently shaken for 30 min. In this type of experiment, optical density was measured at 590 nm. Percentage viability was calculated compared with untreated control (100% viability).

For the MTT assays, MCF-7 and MDA-MB-468 cancer breast cells (~6000 cells/well) were seeded in 96-well plates, using DMEM medium as described previously. Twenty-four hours after plating, various concentrations of TiO_2 sol were added in the appropriate samples, and the samples were irradiated, using UV-A light (wavelength 350 nm), for 20 min. The cells were further cultured for 48 h. The experiment was repeated several times in order to determine the minimal time of UV-activation of titania solutions and the optimal concentration of TiO_2. When the appropriate conditions were selected, the experiment for testing titania effects was repeated at least five times, in quadruplicates. In all instances, similar effects were observed.

2.5. Western blotting

For analysis of caspase-3-mediated PARP cleavage, cells were scraped into PBS, re-suspended in CHAPS buffer containing 1% (v/v) protease inhibitor cocktail (Sigma), and lysed. Protein concentration was determined by the BRADFORD colorimetric assay (PIERCE). Equal amounts of total protein of cell lysates were separated by SDS-PAGE, transferred to HYBOND-ECL nitrocellulose membranes (AMERSHAM). Membranes were probed with anti-PARP antibody (CELL SIGNALLING). Proteins were detected by ECL-detection system (PIERCE) after incubation with horseradish peroxidase-conjugated secondary antibodies (AMERSHAM). To ensure equal amounts of protein loading, the blots were stripped (RE-BLOT PLUS Western Blot Stripping Solution, CHEMICON) and re-probed with anti-β-tubulin monoclonal antibodies. Results were obtained from three independent experiments.

2.6. Statistical analysis

Statistically significant differences between values were evaluated by one-way ANOVA in SPSS program as appropriate. A p value below 0.05 was considered statistically significant.

3. Results

3.1. Photocatalyst characterization

The pH of the titania sol was 1.5 and its transmittance spectrum is shown in Fig. 1. In order to estimate the band gap transition, we have calculated the absorbance $\alpha = 100/\log(T)$ and plotted $(ah\nu)^{1/2}$ vs. $h\nu$ (see inset in Fig. 1), which accounts for an indirect band gap transition which is generally accepted for TiO_2 [32]. Extrapolating the linear part of the $(ah\nu)^{1/2}$ curve at low and high energies we estimated the energy band gap from the crosslinking point of the two lines, equal to 3.28 eV (see inset in Fig. 1). This value is very close to that of the crystalline anatase structure (3.25 eV) [33]. The marginal blue shift of the energy gap, for 0.03 eV, could be due to the emergence of quantum size effects, observable only for very small nanoparticles [34]. The absorption data exclude the possibility that the sol has the amorphous structure since the energy gap, in such a case, should be significantly larger, at about 3.5 eV. In fact the absorption threshold has been defined as an easy and reliable technique for the determination of the structural phase in sol–gel processed titania films [35].

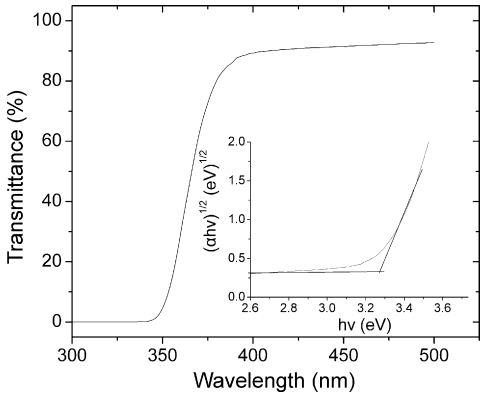

Fig. 1. UV–visible transmittance spectrum of the titania sol. Inset figure presents the photon energy dependence of $(ah\nu)^{1/2}$ (α = absorbance) where from band gap of the titania nanoparticles is estimated.

The material was further structurally characterized by micro-Raman spectroscopy, verifying the results of the transmission spectra. The Raman spectrum of the as-prepared sol on the film is shown in Fig. 2. For comparison, the spectrum of the titania sol after annealing the film at 450 °C for 2 h, is also shown. The Raman spectra show that, upon calcination, the sol nanoparticles collide forming quite large anatase nanocrystals. The frequency and the width of the Raman lines are in agreement with those observed for large nanoparticles with a size above 10 nm [1]. The Raman spectra of the as grown films present close similarities in the number and relative intensities of the peaks with those obtained after calcination, which verifies that the sol is stabilized in the anatase structure, in agreement with the optical results. However, significant shifts and broadenings of the Raman lines in the as-prepared sol are observed due to drastic phonon confinement effects on very small titania nanocrystals. From the peak position (161.8 cm^{-1}) and linewidth (41 cm^{-1}) of the strongest peak, we have estimated a mean crystalline size as low as 2 nm, applying the phonon confinement model. Such small titania anatase nanocrystals have been examined by Raman spectroscopy [35,36], showing similar spectroscopic characteristics. Peaks at 923 and 1053 cm^{-1} are attributed

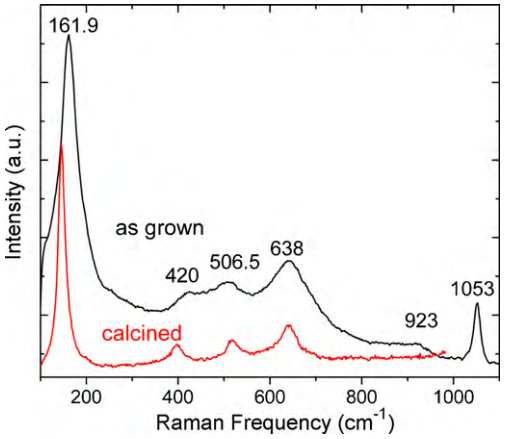

Fig. 2. Raman spectra of the anatase sol particles before and after calcinations at 450 °C for 2 h. Shift and broadening of the Raman lines in the as grown sol are due to drastic phonon confinement in the nanoparticles boundaries.

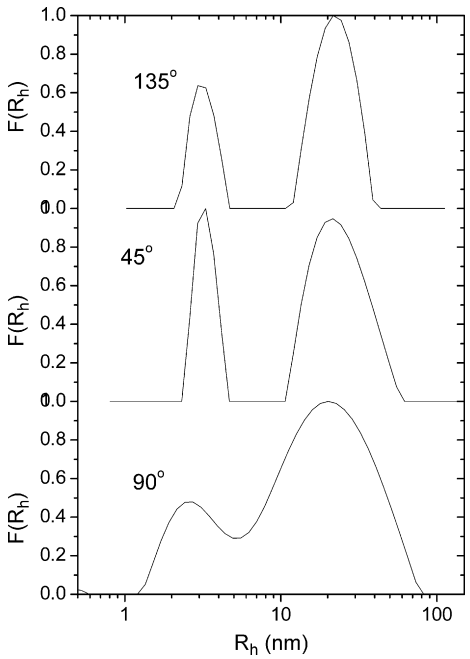

Fig. 3. Distribution of the hydrosol hydrodynamic radii R_h at different scattering angles. Two distinct scattering centers are verified with average size $2R_h$ equal to 5–6 and 40–45 nm, correspondingly.

to ν(N–(OH)) and $\nu_{1s}(NO_3)$ vibrations of the HNO_3 acid in the sol [37].

In Fig. 3, the distribution of hydrodynamic radii at 90° for the mature hydrosol is shown. Two distinct diffusing species are present after analysis and conversion to intensity weighted hydrodynamic radii distributions. The first one, with a mean hydrodynamic radius of 2.6 nm and narrow distribution is attributed to single titania nanoparticles, while the other with a mean hydrodynamic radius of approximately 20 nm and a broad distribution is related to nanoparticle aggregates. Since large aggregates scatter more light than the small ones, in this particular diagram the "apparent concentration" of larger aggregates is considerably overestimated. Under these conditions, it is rational that the number of small nanoparticles (2–3 nm) is significantly higher than the number of larger aggregates (~20 nm). The two distinct scattering centers are verified with dynamic light scattering at different angles (45 and 135°) where the distribution functions are very well separated and the relative integrated intensities of the two peaks are significantly different. Apparent hydrodynamic radius obtained by DLS is certainly bigger than particle radius obtained by Raman scattering, as generally expected [38].

3.2. Effects of photoexcited TiO_2 nanoparticles on the cell cycle

The effects of titania nanoparticles and UV irradiation on the cell cycle of two different human breast cancer cell lines the MDA-MB-468 and MCF-7 were examined by using propidium iodide (PI) staining and flow cytometric (FACScan) analysis. The MCF-7 line retains several characteristics of differentiated mammary epithelium including ability to process estradiol via cytoplasmic estrogen receptors and the capability of forming domes [39]. On the contrary, the MDA-MB-468 cell line displays stem-cell-like characteristics and enhanced tumorigenicity and metastasis *in vivo* [39]. Since we intend to explore if activated-TiO_2 nanoparticles have an effect on specific phases of the cell cycle, cells were not synchronized by serum deprivation before treatment with TiO_2 nanoparticles. In addition, it is known that cellular stresses such as serum deprivation affect cell behaviour which is dependent to a great degree on the nutrients and growth factors found in the environment. Finally, *in vivo*, in a proliferating cell population, cells are not synchronized. The effects of TiO_2 nanoparticles on the cell cycle are presented in Fig. 4. The obtained data thus far indicate a selective action of the titania photocatalysts on the highly malignant MDA-MB-468 cells. Upon irradiation, we obtained experimental evidence that especially the MDA-MB-468 breast epithelial cancer cells were seriously affected, whereas MCF-7 cells were not significantly affected by this treatment. The effect of the TiO_2 was unraveled by detailed examination of the peaks of the diagrams and comparison of the peaks obtained from MCF-7 and MDA-MB-468 cells. The obtained diagrams depicted the phase of the cell cycle focusing on G_1, S and G_2. Interphase (the period of growth) is the period between two sequential cell divisions. During this phase, and especially during the G_1 phase, mRNA, tRNA, ribosomes and proteins are composed [40,41]. The replication of DNA and the synthesis of nuclear histone proteins occur in the synthetic phase (S). G_2 is the phase in which a cell contains two copies of each of the DNA molecules present in the G_1 and is a period of transition before the mitosis (M). The first peak in each diagram gives the number of the cells at the G_1 phase (Fig. 5). The part of the graph between the first two peaks depicts the S phase whereas the second peak corresponds to the G_2 phase. We observed that TiO_2 or UV irradiation treatment of MDA-MB-468 cells resulted in a decrease in the percentage of cells found in G1 phase of the cell cycle (Fig. 4B M2 marker – Histograms b and c) compared to untreated cells (Fig. 4B M2 marker – Histogram a). This effect became more pronounced upon exposure of MDA-MB-468 cells to titania photocatalysts; a 70% decrease in the number of cells found in G1 phase was observed (Fig. 4B M2 marker – Histograms d). In contrast, MCF-7 cells were not affected by any treatment (Fig. 4A (a–d)). Thus, following exposure to photoexcited TiO_2 nanoparticles, the highly malignant MDA-MB-468 cancer cells were decreased in the G1 phase, indicating cell death (necrosis and/or apoptosis), whereas the MCF-7 cells were not affected (Fig. 6). On the contrary, control experiments (not shown) in the presence of UV (in the absence of the photocatalyst) did not reveal significant differences. These results suggest that the stem-like MDA-MB-468 cancer cells exhibit higher sensitivity to photoexcited TiO_2 nanoparticles-induced cell death compared to the more differentiated MCF-7 cells.

3.3. Effects of photoexcited TiO_2 nanoparticles on cell viability

The dose effect of TiO_2 nanoparticles on MCF-7 and MDA-MB-468 cell survival were also evaluated using the MTT assay. Cells were incubated with increasing concentrations of TiO_2 for 48 h and cell viability was determined. The obtained results are summarized in Fig. 7 which shows the percentage of cell viability as a function of the photocatalyst concentration. The cell viability was calculated as follows:

$$\text{Cell viability}\,(\%) = \frac{\overline{\text{ABS}}_{\text{treated}}}{\overline{\text{ABS}}_{\text{untreated}}} \cdot 100\%$$

where, $\overline{\text{ABS}}_{\text{treated}}$ and $\overline{\text{ABS}}_{\text{untreated}}$ are the mean absorption values at 590 nm for the treated and untreated samples, respectively.

A relative cell toxicity resulting from the photocalyst TiO_2 alone was confirmed for both the MDA-MB-468 and the MCF-7 cells. This effect strongly depends on the titania concentration and is particularly evident in the case of the MDA-MB-468 cells. In fact, a gradual reduction of cell viability was observed (Fig. 7A), as the concentration of untreated TiO_2 increased. An amount of TiO_2, equal to 16 μM was "toxic" since it resulted in the death of 50% of MDA-MB-468 cells whereas viability of MCF-7 cells was less affected, since at this concentration, the survival rate of MCF-7 cells is approximately 80%. The effect of the UV irradiation, on cell viability presented in

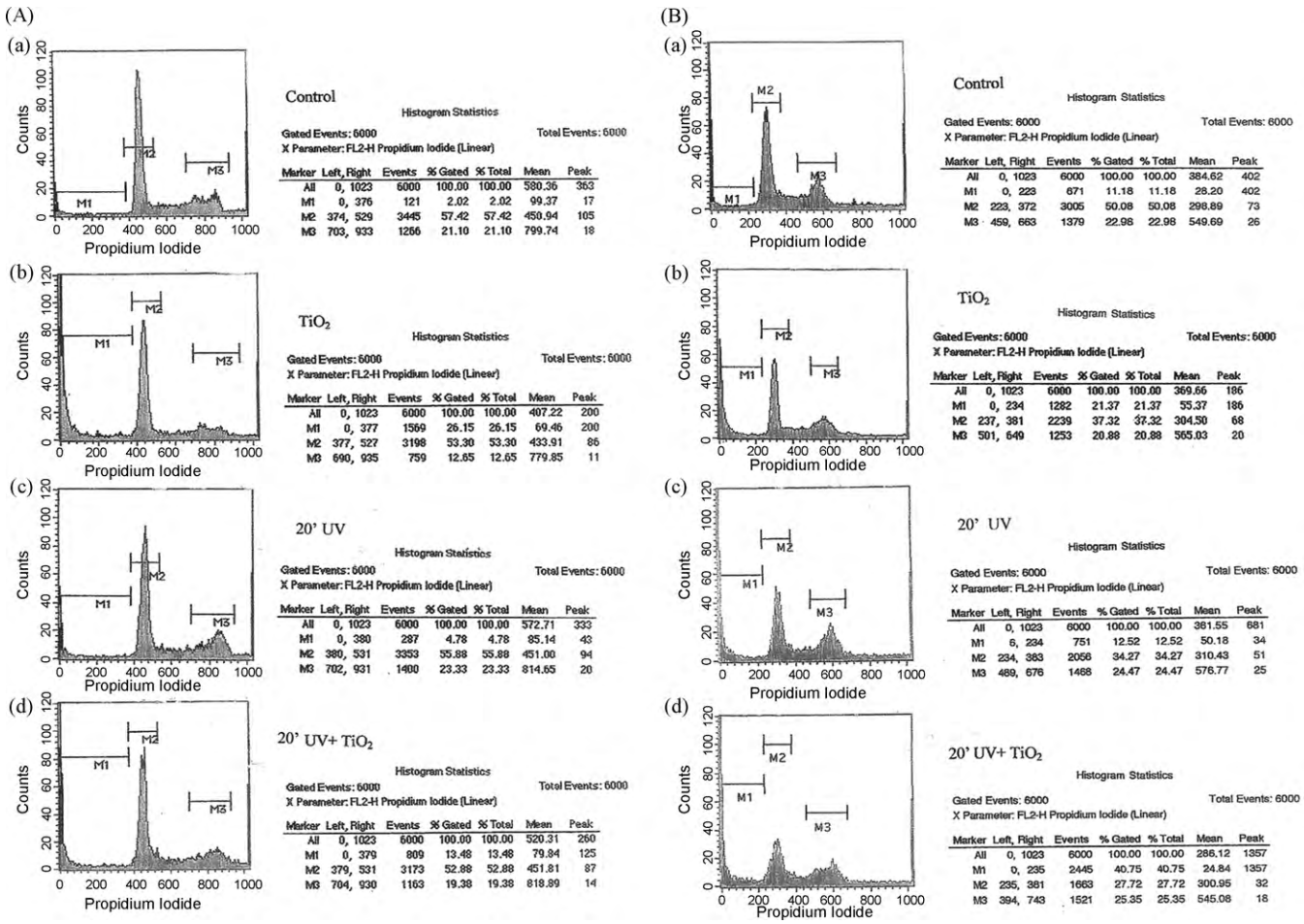

Fig. 4. Effect of photoexcited TiO_2 nanoparticles on the cell cycle. MDA-MB-468 and MCF-7 cells were treated with 15 μM TiO_2, UVA-irradiated for 20 min and incubated for 48 h. Cells were then fixed and DNA quantification was performed by PI staining and flow cytometric analysis. (A) FACS analysis of MCF-7 cells. Six thousand events per sample were counted. The M2 gate demarcates the G1 cell population and the M3 gate the G2/M cell population: (a) control cells (untreated), (b) cells treated with 15 μM TiO_2, (c) cells treated with UV-A, (d) cells treated with UV-irradiated titania. (B) FACS analysis of MDA-MB-468 cells. Six thousand events per sample were counted. (a) Control cells (untreated) (b) cells treated with 15 μM TiO_2 (c) cells treated with UV-A (d) cells treated with UV-irradiated titania.

Fig. 7B reveals a completely different pattern. The UV irradiation by itself has a minor effect on cell viability (about 10% without TiO_2, data not shown). Our results indicate that the cytotoxic effect of UV-irradiated TiO_2 on MDA-MB-468 cells was also concentration dependent. The effect of photo-activated-TiO_2 on MDA-MB-468 cell survival is highlighted at concentration between 10 and 16 μM of TiO_2. A significant loss of cell viability (approximately 50–60% viability) was observed at concentrations between 10 and 16 μM of TiO_2 (Fig. 7B) whereas under the same conditions, the viability of MCF-7 is around 75–85% (Fig. 7B). Thus, our results show that the highly malignant MDA-MB-468 cancer cells are more susceptible to TiO_2 nanoparticles- or UV-activated-TiO_2 nanoparticles-induced cell death compared to the MCF-7 cells.

3.4. *Effect of photoexcited TiO_2 nanoparticles on caspase-3-mediated PARP cleavage*

The process leading to cell apoptosis is executed by the family of caspases, including caspase-3. Activation of caspases contributes to the morphological and functional changes associated with apoptosis [42,43]. One of the main cleavage targets of caspase-3 *in vivo* is PARP, a 113 kDa nuclear poly (ADP-ribose) polymerase, appears to be involved in DNA repair in response to environmental stress [42,44,45]. Cleavage of PARP facilitates cellular disassembly and serves as a marker of cells undergoing apoptosis [46]. To determine whether the observed reduced cell viability was the result of apoptotic induction, PARP cleavage was examined by Western blot analysis in cells treated with UV-activated titania. Lysates of cells treated for 24 h with 200 nM staurosporine or serum-depleted cells were used as positive control for induction of PARP cleavage. As shown in Fig. 8A and B, in MDA-MB-468 cells UV-A light (without TiO_2 nanoparticles) slightly up-regulated PARP cleavage compared with the control group. However, when the cells were treated with TiO_2 nanoparticles or photoexcited TiO_2 nanoparticles, PARP cleavage significantly increased (Fig. 8A and B), confirming that TiO_2

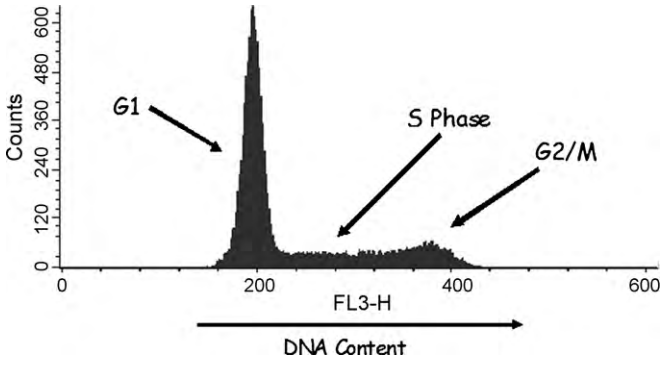

Fig. 5. Typical flow cytometric profile of the DNA content in cells stained with PI.

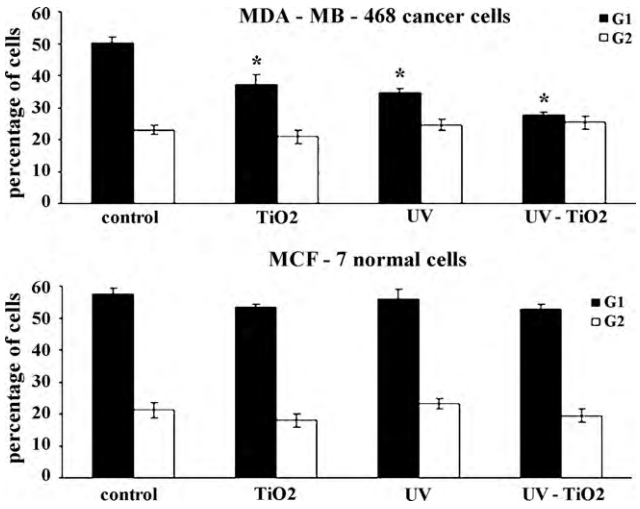

Fig. 6. Comparative diagrams of the percentage of the cells existing in G_1 and G_2 phase of the cell cycle. Data represent the means ± SD from four independent experiments. *$P < 0.05$ as compared to control (untreated) cells.

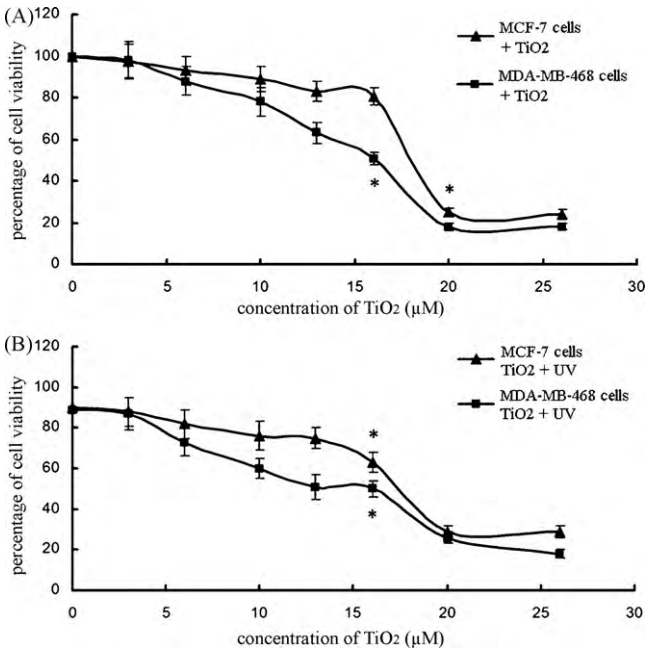

Fig. 7. Effect of photoexcited TiO_2 nanoparticles on cell viability. MCF-7 and MDA-MB-468 cancer breast epithelial cells were treated with increasing concentrations of TiO_2, UVA-irradiated for 20 min and incubated for 48 h. Cell viability was determined by the MTT assay. (A) Effect of TiO_2 concentration on cell viability. (B) Effect of the concentration of UVA-irradiated TiO_2 on cell viability. Data represent the means ± SD from five independent experiments. *$P < 0.05$ as compared to control (untreated) cells.

nanoparticles treatment triggers apoptosis in MDA-MB-468 cells. Under the same conditions, in MCF-7 cells, PARP cleavage was not detected (Fig. 8C and D). Taken together our results indicated that TiO_2 nanoparticles alone or photoexcited TiO_2 nanoparticles induced significant apoptosis especially in MDA-MB-468 cells.

4. Discussion

TiO_2 nanoparticles are widely used for industrial and medical applications [47,48]. Since nanoparticles can interact with cell membranes and cellular organelles in a manner not totally understood there are increasing concerns about the adverse health effects of TiO_2 nanoparticles. Until now, data showing the cytotoxic effects and related mechanism of TiO_2 in cultured cells have been inconsistent. In this study, we investigated the cell toxicity effects of TiO_2 nanoparticles on two breast cancer cell lines the MDA-MB-468 and MCF-7. Our results showed that TiO_2 nanoparticles possess cell-specific toxicity, depending on the concentration of the particular particles. We found that concentrations of TiO_2 or photoexcited TiO_2 nanoparticles, between 10 and 16 μM, have low toxicity to MCF-7 cells. However, under the same conditions TiO_2 nanoparticles induced significant cytotoxicity in MDA-MB-468 cells.

These findings are in agreement with many recent publications. Specifically, Kiss et al. [49] reported that TiO_2 nanoparticles exerted significant and cell-type dependent effects on cellular functions such as viability, proliferation and apoptosis in human skin-derived cells *in vitro*. Thevenot et al. [50] demonstrated that TiO_2 nanoparticles have cell-specific toxicity, depending on the concentration of the particular particles. TiO_2 particle-mediated cell toxicity is potentially due to particle–cell interactions possibly related to the surface properties of the TiO_2 particles [51]. It has been reported

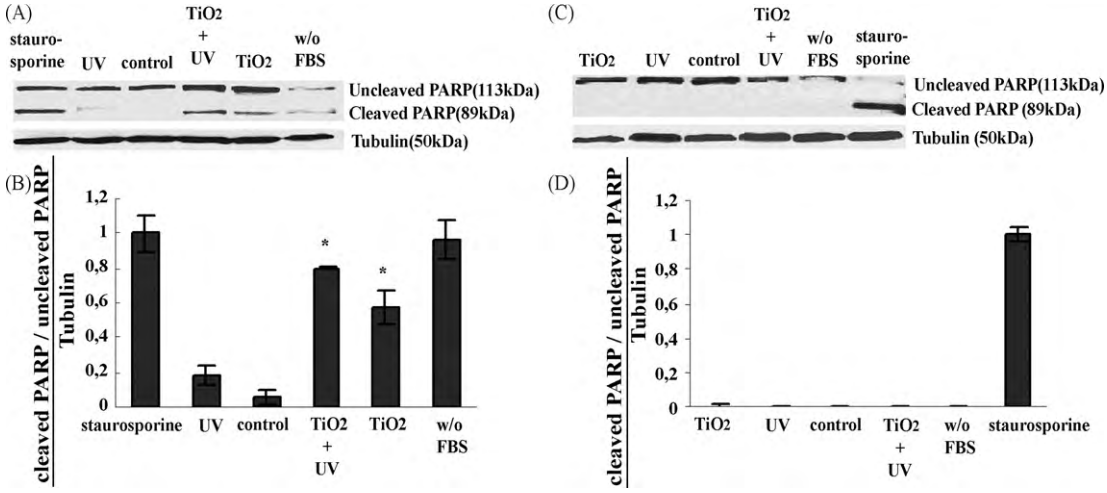

Fig. 8. Photoexcited TiO_2 nanoparticles induced caspase-3-mediated PARP cleavage. MDA-MB-468 and MCF-7 cells were treated with 15 μM TiO_2, UV-A-irradiated for 20 min and incubated for 48 h. Cells were then lysed and cell lysates were immunoblotted with anti-PARP antibody. (A and C) Representative Western blots of uncleaved and cleaved PARP. Cells treated with 200 nM staurosporine for 24 h or serum-depleted cells were used as positive control for induction of PARP cleavage. Blots were stripped and re-probed with anti-tubulin antibody to normalize the blots for protein levels. (B and D) Densitometric quantification of cleaved/uncleaved PARP to tubulin levels. Data represent the means ± SD from three independent experiments. *$P < 0.05$ as compared to cleaved/uncleaved PARP/tubulin levels of untreated cells.

in several *in vivo* studies that TiO_2 can travel in the bloodstream via binding to plasma proteins, through the lymphatic system after phagocytosis by macrophages, or to the bone marrow via monocytes [52,53]. The specific interactions between TiO_2 particles and proteins are not well understood. Studies have revealed that TiO_2 particles have a net negative charge (at pH 7) and also bind preferentially to amino acids containing –OH, –NH, and $–NH_2$ in their side chains [54,55]. These observations indicate that TiO_2 particles may react with cell membrane proteins and contribute to cell particle interaction.

Our results indicate that the effect of TiO_2 nanoparticles on cell toxicity is cell-dependent. MCF-7 cells showed no significant response to TiO_2 particles compared to MDA-MB-468 at concentrations as high as 16 μM. These differences may be due to protein composition of the cell membrane and the manner in which membrane proteins interact with the TiO_2 particles. In the case of the MCF-7 cells, weaker particle membrane interactions may explain the insignificant influence and higher survival rates of particle-exposed cells (Fig. 5). In contrast, TiO_2 nanoparticles exert significant influence on MDA-MB-468 cell toxicity, possibly as a result of increased interaction between the TiO_2 particle and the cell membrane. Indeed, MDA-MB-468 cells demonstrating stem-cell-like characteristics (high expression of cancer stem cells (SCCs) markers CD44/CD133 and high functional activity of aldehyde dehydrogenase (ALDH), an enzyme involved in stem cell self-protection, compared to MCF-7 (39). *In vitro*, MDA-MB-468 cells demonstrated increased growth, colony formation, adhesion, migration and invasion. Furthermore, *in vivo*, cells showed enhanced tumorigenicity and metastasis relative to MCF-7 cells [39]. Our results are in agreement with recent findings suggesting that the degree of TiO_2 nanoparticles cytotoxicity is depended on the interactions between TiO_2 nanoparticle and the properties of a particular cancer cell's membrane [50]. Alternatively, the observed low toxicity of TiO_2 on MCF-7 cells could be attributed to the fact that these cells are generally very resistant since they contain a xenobiotic transporter (BCRP) that appears to play a major role in the multidrug resistance. However, it was reported that nano-TiO_2 increased the drug accumulation in target cancer cells and also acted as an effective anti-multidrug-resistant agent to inhibit the relative drug resistance in leukemia cells [56]. Thus, although treatment of cancer MCF-7 cells with TiO_2 nanoparticles had no significant effect on cell viability, it is possible that the effectiveness of photo-activated-TiO_2 nanoparticles on MCF-7 cells will be revealed upon simultaneous treatment of cells with an anticancer drug. Synergistic action of photo-activated-TiO_2 nanoparticles and anticancer drug to drug-resistant tumor cells may further provoke significant changes to the cellular membrane of the cancer cell thus enhancing the chemotherapy effect for the targeted tumor treatment.

We also examined whether reduced cell viability is related to apoptotic cell death. Western blotting for PARP revealed that TiO_2-induced MDA-MB-468 cell death is associated, at least in part, with apoptosis. These results are in agreement with recent publications reporting increased apoptotic induction in TiO_2 exposed H1299 non-small cell lung cancer cells [57] and the skin melanoma A-375 cells [58].

Recently, intensive efforts are focused on the production and the use of targeted cytotoxicity of TiO_2 nanoparticles for photodynamic therapy of cancers. It was reported that modification of TiO_2 nanoparticles with some biomolecules that can specifically bind to cancer cells improved selectivity and efficiency of TiO_2 to destroy cancer cells [59]. Rozhkova et al. [60] demonstrated that TiO_2 particles covalently tethered to an antibody via a dihydroxybenzene bivalent linker, which enables absorption of a visible part of the solar spectrum by the nanobio hybrid, specifically induced antiglioblastoma cell phototoxicity. The phototoxicity is mediated by reactive oxygen species (ROS) that initiate programmed death of the cancer cell.

Oxidative stress is known to induce cellular death by apoptosis or necrosis [61]. The production of reactive oxygen species, i.e. oxidative stress has been proven to increase with the nano-TiO_2 concentration [17,62] even without ultraviolet radiation [16]. In the presence of ultraviolet (UV) light with a wavelength <390 nm, nano-TiO_2 produce electrons and holes leading subsequently to the formation of ROS such as hydroxyl radicals, superoxides and hydrogen peroxide. These oxygen species are highly reactive with cell membranes and the cell interior, including DNA, with damaged areas depending on particle location upon excitation. Such oxidative reactions affect cell rigidity and chemical arrangement of surface structures, leading to cell toxicity [50,63–65]. Molecular scavengers of both hydrogen peroxide and hydroxyl radicals, such as catalase and *N*-acetylcysteine could effectively diminish cell death when added to cell samples. These findings provide evidence that hydroxyl radicals and hydrogen peroxide play a role in cell death [66–68].

It has been proposed that cell damage induced by nanoparticles occurs in two stages. In the first stage, binding of TiO_2 nanoparticles to cell membrane is followed by oxidative damage by the photogenerated holes. This leads to permeabilization of the cell membrane, but does not produce a significant decrease in cell viability. The decrease in cell viability, eventually cell death, occurs in a second stage as a result of leaking intracellular components, or nano-TiO_2 trafficking into the damaged cells that directly attack nuclei and other intracellular components [64]. Thus, oxidant-mediated cell damage may be a relevant cause for the cellular modifications seen in our study and should be investigated further since additional insights are required into intracellular signalling resulting in cell death induced by photoexcited TiO_2 nanoparticles. According to our results, TiO_2 nanoparticles had no significant effects on MCF-7 cell survival, whereas the highly malignant MDA-MB-468 cells were seriously affected. It is then possible that also in humans, TiO_2 might only be toxic to advanced cancers and not cancers at the initial stages (which would be composed of something like MCF-7 cells).

Nano-TiO_2 can induce cancer cell apoptosis and be used as a photosensitizer in photodynamic therapy for endobronchial and esophageal cancers [69]. The observed photocatalytic killing effect of TiO_2 nanoparticles on human epithelial breast carcinoma MDA-MB-468 cells further supports the idea of cancer treatment using TiO_2 nanoparticles and light irradiation. Under these conditions, it could be adapted to an anticancer modality by the local or regional treatment of the tumor with TiO_2 nanoparticles, followed by light irradiation focusing on the tumor. Although UVA light cannot penetrate the human body, cancer cells can be selectively killed as the light beam can be introduced via a fiber optic near a tumor region, where titanium oxide photocalysts are also applied by simple injection [2]. Thus, it may be possible that this modality will be applied to several human tumors in the future.

5. Conclusion

Focusing our research on the photocatalytic activity of titanium dioxide (TiO_2) aqueous sols, prepared using the sol–gel technique, we established the possible use of the material as an anticancer agent. Cultured MCF-7 and MDA-MB-468 breast cancer epithelial cells, were irradiated, using UV-A light (wavelength 350 nm) for 20 min, in the presence of nanostructured titania. The effects of photocatalytic treatment on the cell cycle and cell viability were analyzed and identified, thus obtaining preliminary evidence about selective destruction of the MDA-MB-468 cancer breast epithelial cells by both TiO_2 nanoparticles and UV-activated titania.

The photoexcited TiO_2 sol containing anatase nanoparticles can remarkably induce apoptosis in MDA-MB-468 cells. Although the precise molecular mechanism involved in the preferential death of these cancer cells is under intensive investigation and needs additional exploration, the obtained results indicate that the anti-tumor process of apoptosis is closely associated with increased caspase-3-mediated PARP cleavage. Since UVA irradiation is harmful for cells, further optimization of the photocatalytic cancer treatment effective for targeted cancer therapy is possible, by tuning the TiO_2 nanoparticles size or surface engineering the nanoparticles and inducing activation using visible-light. Furthermore, examination of the cancer killing effect of photo-activated-TiO_2 nanoparticles, *in vivo*, in animal models with cancer, is required to unravel the specificity of anti-tumor effect of photoexcited TiO_2 nanoparticles.

Acknowledgments

The authors are thankful to the Greek General Secretariat for Research and Technology for providing financial support though National Projects PEP Attikis (ATT-25) and 4.5/4.4.1 Competitiveness/Infrastructure-EPAN YPODOMON.

References

[1] A.I. Kontos, A.G. Kontos, D.S. Tsoukleris, G.D. Vlachos, P. Falaras, Superhydrophilicity and photocatalytic property of nanocrystalline titania sol–gel films, Thin Solid Films 515 (2007) 7370–7375.
[2] A. Fujishima, K. Hashimoto, T. Watanabe, TiO_2 Photocatalysis, Fundamentals and Applications, BKC, Inc., Tokyo, 1999.
[3] Y.T. Sul, C.B. Johansson, S. Petronis, A. Krozer, Y. Jeong, A. Wennerberg, T. Albrektsson, Characteristics of the surface oxides on turned and electrochemically oxidized pure titanium implants up to dielectric breakdown: the oxide thickness, micropore configurations, surface roughness, crystal structure and chemical composition, Biomaterials 23 (2002) 491–501.
[4] H. Choi, E. Stathatos, D.D. Dionysiou, Sol–gel preparation of mesoporous photocatalytic TiO_2 films and TiO_2/Al_2O_3 composite membranes for environmental applications, Applied Catalysis B: Environmental 63 (2006) 60–67.
[5] T. Phenrat, G.V. Lowry, Physicochemistry of polyelectrolyte coatings that increase stability, mobility, and contaminant specificity of reactive nanoparticles used for groundwater remediation, Nanotechnology Applications for Clean Water (2009) 249–267.
[6] L. Brunet, D.Y. Lyon, E.M. Hotze, P.J.J. Alvarez, M.R. Wiesner, Comparative photoactivity and antibacterial properties of C_{60} fullerenes and titanium dioxide nanoparticles, Environmental Science and Technology 43 (12) (2009) 4355–4360.
[7] G. Balasubramanian, D.D. Dionysiou, M.T. Suidan, I. Baudin, J.-M. Laîné, Evaluating the activities of immobilized TiO_2 powder films for the photocatalytic degradation of organic contaminants in water, Applied Catalysis B: Environmental 47 (2004) 73–84.
[8] E.R. Bandala, S. Gelover, M.T. Leal, C. Arancibia-Bulnes, A. Jimenez, C.A. Estrada, Solar photocatalytic degradation of Aldrin, Catalysis Today 76 (2002) 189–199.
[9] A. Fujishima, T.N. Rao, D.A. Tryk, Titanium dioxide photocatalysis, Journal of Photochemistry and Photobiology C: Photochemical Review 1 (2000) 1–21.
[10] J.A. Rengifo-Herrera, C. Pulgarin, Photocatalytic activity of N, S co-doped and N-doped commercial anatase TiO_2 powders towards phenol oxidation and *E. coli* inactivation under simulated solar light irradiation, Solar Energy 84 (2010) 37–43.
[11] D. Gumy, A.G. Rincon, R. Hajdu, C. Pulgarin, Solar photocatalysis for detoxification and disinfection of water: different types of suspended and fixed TiO_2 catalysts study, Solar Energy 80 (2006) 1376–1381.
[12] Q. Zhang, Y. Kusaka, K. Sato, K. Nakakuki, N. Kohyama, K. Donaldson, Differences in the extent of inflammation caused by intratracheal exposure to three ultrafine metals: role of free radicals, Journal of Toxicology and Environmental Health A 53 (1998) 423–438.
[13] K. Donaldson, D. Brown, A. Clouter, R. Duffin, W. MacNee, L. Renwick, L. Tran, V. Stone, The pulmonary toxicology of ultrafine particles, Journal of Aerosol Medicine: The Official Journal of the International Society for Aerosols in Medicine 15 (2002) 213–220.
[14] C.M. Sayes, R. Wahi, P.A. Kurian, Y. Liu, J.L. West, K.D. Ausman, D.B. Warheit, V.L. Colvin, Correlating nanoscale titania structure with toxicity: a cytotoxicity and inflammatory response study with human dermal fibroblasts and human lung epithelial cells, Toxicological Sciences: An Official Journal of the Society of Toxicology 92 (2006) 174–185.
[15] M.L. Wang, R. Tuli, P.A. Manner, P.F. Sharkey, D.J. Hall, R.S. Tuan, Direct and indirect induction of apoptosis in human mesenchymal stem cells in response to titanium particles, Journal of Orthopaedic Research: Official Publication of the Orthopaedic Research Society 21 (2003) 697–707.
[16] D.P. Pioletti, H. Takei, S.Y. Kwon, D. Wood, K.L. Sung, The cytotoxic effect of titanium particles phagocytosed by osteoblasts, Journal of Biomedical Materials Research 46 (1999) 399–407.
[17] T.C. Long, J. Tajuba, P. Sama, N. Saleh, C. Swartz, J. Parker, S. Hester, G.V. Lowry, B. Veronesi, Nanosize titanium dioxide stimulates reactive oxygen species in brain microglia and damages neurons in vitro, Environmental Health Perspectives 115 (2007) 1631–1637.
[18] E. Osano, J. Kishi, Y. Takahashi, Phagocytosis of titanium particles and necrosis in TNF-alpha-resistant mouse sarcoma L929 cells, Toxicology In Vitro: An International Journal Published in Association with BIBRA 17 (2003) 41–47.
[19] J.J. Wang, B.J. Sanderson, H. Wang, Cyto- and geno-toxicity of ultrafine TiO_2 particles in cultured human lymphoblastoid cells, Mutation Research 628 (2007) 99–106.
[20] N.P. Huang, M.H. Xu, C.W. Yuan, R.R. Yu, The study of the photokilling effect and mechanism of ultrafine TiO_2 particles on U937 cells, Journal of Photochemistry and Photobiology A: Chemistry 108 (1997) 229–233.
[21] A.P. Zhang, Y.P. Sun, Photocatalytic killing effect of TiO_2 nanoparticles on LS-174-T human colon cancer cells, World Journal of Gastroenterology 10 (2004) 3191–3193.
[22] M. Song, R. Zhang, Y. Dai, F. Gao, H. Chi, G. Lv, B. Chen, X. Wang, The in vitro inhibition of multidrug resistance by combined nanoparticulate titanium dioxide and UV irradiation, Biomaterials 27 (2006) 4230–4238.
[23] C.-H. Xia, B.Q. Wang, Y. Wang, Y.-Q. Liu, G.-Y. Xu, S. Wu, Damaging effects of nanosized TiO_2 on Bel-7402 human liver cancer cell under photoinduce, Journal of Inorganic Materials 21 (2006) 1467–1471.
[24] K. Hirakawa, M. Mori, M. Yoshida, S. Oikawab, S. Kawanishib, Photo-irradiated titanium dioxide catalyzes site specific DNA damage via generation of hydrogen peroxide, Free Radical Research 38 (2004) 439–447.
[25] Y. Kubota, T. Shuin, C. Kawasaki, M. Hosaka, H. Kitamura, R. Cai, H. Sakai, K. Hashimoto, A. Fujishima, Photokilling of T-24 human bladder cancer cells with titanium dioxide, British Journal of Cancer 70 (1994) 1107–1111.
[26] A.L. Linseblgler, G. Lu, J.T. Yates Jr., Photocatalysis on TiO_2 surfaces: principles, mechanisms, and selected results, Chemical Review 95 (1995) 735–758.
[27] H. Sakai, E. Ito, R. Cai, T. Yoshioka, K. Hashimoto, A. Fujishima, Intracellular Ca^{2+} concentration change of T24 cell under irradiation in the presence of TiO_2 ultrafine particles, Biochimica et Biophysica Acta 1201 (1995) 259–265.
[28] A. Meristoudi, S. Pispas, N. Vainos, Self-assembly in solutions of block and random copolymers during metal nanoparticle formation, Journal of Polymer Science: Part B: Polymer Physics 46 (2008) 1515–1524.
[29] Z. Darzynkiewicz, S. Bruno, G. Del Bino, W. Gorczyca, M.A. Hotz, P. Lassota, F. Traganos, Features of apoptotic cells measured by flow cytometry, Cytometry 13 (1992) 795–808.
[30] T. Rapid Mosmann, Colorimetric assay for cellular growth and survival: application to proliferation and cytotoxicity assays, Journal of Immunological Methods 65 (1983) 55–63.
[31] J.A. Plumb, Cell sensitivity assays: the MTT assay, Methods in Molecular Medicine 88 (2004) 165–169.
[32] A.I. Kontos, A.G. Kontos, Y.S. Raptis, P. Falaras, Nitrogen modified nanostructured titania: electronic, structural and visible-light photocatalytic properties, Physica Status Solidi (RRL) 2 (2008) 83–85.
[33] A. Welte, C. Waldauf, C. Brabec, P.J. Wellmann, Application of optical absorbance for the investigation of electronic and structural properties of sol–gel processed TiO_2 films, Thin Solid Films 516 (2008) 7256–7725.
[34] N. Serpone, D. Lawless, R. Khairutdinov, Size effects on the photophysical properties of colloidal anatase TiO_2 particles: size quantization versus direct transitions in this indirect semiconductor? Journal of Physical Chemistry 99 (1995) 16646–16654.
[35] K.R. Zhu, M.S. Zhang, Q. Chen, Z. Yin, Size and phonon-confinement effects on low-frequency Raman mode of anatase TiO_2 nanocrystal, Physics Letters A 340 (2005) 220–227.
[36] V. Swamy, A. Kuznetsov, L.S. Dubrovinsky, R.A. Caruso, D.G. Shchukin, B.C. Muddle, Finite-size and pressure effects on the Raman spectrum of nanocrystalline anatase TiO_2, Physical Review B 71 (2005) 184302.
[37] C.E. Lund Myhre, H. Grothe, A.A. Gola, C.J. Nielsen, Optical constants of HNO_3/H_2O and $H_2SO_4/HNO_3/H_2O$ at low temperatures in the infrared region, Journal of Physical Chemistry A 109 (2005) 7166–7171.
[38] L. Kvitek, R. Prucek, A. Panácek, R. Novotny, J. Hrbac, R. Zboril, Polyacrylate-assisted synthesis of stable copper nanoparticles and copper(I) oxide nanocubes with high catalytic efficiency, Journal of Materials Chemistry 15 (2005) 1099–1105.
[39] A. Croker, D. Goodale, J. Chu, C. Postenka, B. Hedley, D. Hess, A. Allan, High aldehyde dehydrogenase and expression of cancer stem cell markers selects for breast cancer cells with enhanced malignant and metastatic ability, Journal of Cellular and Molecular Medicine 13 (2009) 2236–2252.
[40] J. Darnell, H. Lodish, D. Baltimore, Molecular Cell Biology, Scientific American Books, 1986.
[41] A.H. Wyllie, Apoptosis, an overview, British Medical Bulletin 53 (1997) 451–465.
[42] H. Hui, F. Dotta, U. Di Mario, R. Perfetti, Role of caspases in the regulation of apoptotic pancreatic islet beta-cells death, Journal of Cellular Physiology 200 (2004) 177–200.
[43] D.W. Nicholson, A. Ali, N.A. Thornberry, J.P. Vaillancourt, C.K. Ding, M. Gallant, Y. Gareau, P.R. Griffin, M. Labelle, Y.A. Lazebnik, N.A. Munday, S.M. Raju, M.E. Smulson, T.T. Yamin, V.L. Yu, D.K. Miller, Identification and inhibition of the ICE/CED-3 protease necessary for mammalian apoptosis, Nature 376 (1995) 17–18.

[44] M. Tewari, L.T. Quan, L.T. O'Rourke, S. Desnoyers, Z. Zeng, D.R. Beidler, G.G. Poirier, G.S. Salvesen, V.M. Dixit, Yama/CPP32 beta, a mammalian homolog of CED-3, is a CrmA-inhibitable protease that cleaves the death substrate poly (ADP-ribose) polymerase, Cell 81 (1995) 801–809.
[45] M.S. Satoh, T. Lindahl, Role of poly (ADP-ribose) formation in DNA repair, Nature 356 (1992) 356–358.
[46] F.J. Oliver, G. de la Rubia, V. Rolli, M.C. Ruiz-Ruiz, G. de Murcia, J.M. Murcia, Importance of poly(ADP-ribose) polymerase and its cleavage in apoptosis, Lesson from an uncleavable mutant, The Journal of Biological Chemistry 273 (1998) 33533–33539.
[47] K. Arshak, D. Morris, A. Arshak, O. Korostynska, E. Jafer, Evaluating the suitability of thick-film TiO_2 capacitors for use in a wireless pressure measurement system, Materials Science and Engineering 26C (2006) 1077–1081.
[48] F. Agar, I. Justicia, R. Gerbasi, G. Battiston, N. McSporran, A. Figueras, RBS analysis of substoichiometric TiO_2-anatase thin films for visible light photocatalysis, Nuclear Instruments and Methods in Physical Research 249B (2006) 490–492.
[49] B. Kiss, T. Biro, G. Czifra, B. Toth, Z. Kertesz, Z. Szikszai, A. Kiss, I. Juhasz, C. Zouboulis, J. Hunyadi, Investigation of micronized titanium dioxide penetration in human skin xenografts and its effect on cellular functions of human skin-derived cells, Experimental Dermatology 17 (2008) 659–667.
[50] P. Thevenot, Jai Cho, D. Wavhal, R. Timmons, L. Tang, Surface chemistry influences cancer killing effect of TiO_2 nanoparticles, Nanomedicine: Nanotechnology, Biology and Medicine 4 (2008) 226–236.
[51] D. Warheit, T. Webb, K. Reed, S. Frerichs, C. Sayes, Pulmonary toxicity study in rats with three forms of ultrafine-TiO_2 particles: differential responses related to surface properties, Toxicology 230 (2007) 90–104.
[52] R. Urban, J. Jacobs, M. Tomlinson, J. Gavrilovich, J. Black, M. Peoc'h, Dissemination of wear particles to the liver, spleen, and abdominallymph nodes of patients with hip or knee replacement, The Journal of Bone and Joint Surgery 82A (2000) 457–477.
[53] D. Olmedo, M. Guglielmotti, R. Cabrini, An experimental study of the dissemination of titanium and zirconium in the body, Journal of Materials Science Materials in Medicine 13 (2002) 793–796.
[54] E. Topoglidis, B. Discher, C. Moser, P. Dutton, J. Durrant, Functionalizing nanocrystalline metal oxide electrodes with robust synthetic redox proteins, Chembiochem 4 (2003) 1332–1339.
[55] T. Tran, A. Nosaka, Y. Nosaka, Adsorption and photocatalytic decomposition of amino acids in TiO_2 photocatalytic systems, Journal of Physical Chemistry B 110 (2006) 25525–25531.
[56] M. Song, R. Zhanga, Y. Dai, F. Gao, H. Chi, G. Lv, B. Chen, X. Wang, The in vitro inhibition of multidrug resistance by combined nanoparticulate titanium dioxide and UV irradiation, Biomaterials 27 (2006) 4230–4238.
[57] Y. Lee, S. Yoon, H. Yoon, K. Lee, H. Yoon, J. Lee, C. Song, Inhibitor of differentiation 1 (Id1) expression attenuates the degree of TiO_2-induced cytotoxicity in H1299 non-small cell lung cancer cells, Toxicology Letters 189 (2009) 191–199.
[58] J. Seo, H. Chung, M. Kim, J. Lee, I. Choi, J. Cheon, Development of water-soluble single-crystalline TiO_2 nanoparticles for photocatalytic cancer-cell treatment, Small 3 (2007) 850–853.
[59] J. Xu, Y. Sun, J. Huang, C. Chen, G. Liu, Y. Jiang, Y. Zhao, Z. Jiang, Photokilling cancer cells using highly cell-specific antibody–TiO_2 bioconjugates and electroporation, Bioelectrochemistry 71 (2007) 217–222.
[60] E. Rozhkova, I. Ulasov, B. Lai, N. Dimitrijevic, M. Lesniak, T. Rajh, A high-performance nanobio photocatalyst for targeted brain cancer therapy, Nano Letters 9 (2009) 3337–3342.
[61] V. Gogvadze, S. Orrenius, B. Zhivotovsky, Mitochondria as targets for chemotherapy, Apoptosis 14 (2009) 624–640.
[62] T.C. Long, N. Saleh, R.D. Tilton, G.V. Lowry, B. Veronesi, Titanium dioxide (P25) produces reactive oxygen species in immortalized brain microglia (BV2): implications for nanoparticle neurotoxicity, Environmental Science and Technology 40 (2006) 4346–4352.
[63] Q. Rahman, M. Lohani, E. Dopp, H. Pemsel, L. Jonas, D.G. Weiss, D. Schiffmann, Evidence that ultrafine titanium dioxide induces micronuclei and apoptosis in Syrian hamster embryo fibroblasts, Environmental Health Perspectives 110 (2002) 797–800.
[64] L. Wang, J. Mao, G.H. Zhang, M.J. Tu, Nano-cerium-element doped titanium dioxide induces apoptosis of Bel 7402 human hepatoma cells in the presence of visible light, World Journal of Gastroenterology 13 (29) (2007) 4011–4014.
[65] C.I. Vamanu, M.R. Cimpan, P.J. Høl, S. Sornes, S.A. Lie, N.R. Gjerdet, Induction of cell death by TiO_2 nanoparticles: studies on a human monoblastoid cell line, Toxicology In Vitro 22 (2008) 1689–1696.
[66] T. Uchino, H. Tokunaga, M. Ando, H. Utsumi, Quantitative determination of OH radical generation and its cytotoxicity induced by TiO_2-UVA treatment, Toxicology In Vitro 16 (2002) 629–635.
[67] R. Cai, Y. Kubota, T. Shuin, H. Sakai, K. Hashimoto, A. Fujishima, Induction of cytotoxicity by photoexcited TiO_2 particles, Cancer Research 52 (1992) 2346–2348.
[68] J. Chandra, A. Samali, S. Orrenius, Triggering and modulation of apoptosis by oxidative stress, Free Radical Biology and Medicine 29 (3/4) (2000) 323–333.
[69] R. Ackroyd, C. Kelty, N. Brown, M. Reed, The history of photodetection and photodynamic therapy, Photochemistry and Photobiology 74 (2001) 656–669.